Int. J. Electrochem. Sci., 15 **(2020)** 11102 – 11111, doi: 10.20964/2020.11.75

International Journal of
ELECTROCHEMICAL
SCIENCE
www.electrochemsci.org

Study of Sodium Insertion into Phosphorus-Carbon Composite at Lower Temperatures

Alexander Skundin[*], *Tatiana Kulova, Dmitry Gryzlov and Yulia Kudryashova*

Frumkin Institute of Physical Chemistry and Electrochemistry of the RAS, 31-4 Leninskii ave., 119071 Moscow, Russia
[*]E-mail: askundin@mail.ru

Received: 11 August 2020 / *Accepted:* 13 September 2020 / *Published:* 30 September 2020

The electrochemical behavior of electrodes based on a composite of red phosphorus with modified oxidized graphite (P@MOG) was studied in the temperature range from –40 to +20 °C for the first time. P@MOG composite was synthesized via evaporation-condensation method. The temperature dependence of reversible capacity of P@MOG happened to be rather weak at the temperatures from 20 to –10 °C, whereas at lower temperatures this dependence obeys Arrhenius-kind equation with effective activation energy ca. 34 kJ mole^{-1}.

Keywords: sodium-ion batteries, phosphorus-based materials, negative temperatures, sodium insertion-exaction, activation energy of diffusion

1. INTRODUCTION

Successful development of new high-energy functional materials for sodium-ion batteries allows us to confidently consider the latter as an alternative to lithium-ion batteries. The most promising materials for the negative electrode of a sodium-ion battery in terms of high capacity include phosphorus, the specific theoretical capacity of which amounts to 2596 mAh g^{-1}.

With due account for rather low electronic conductivity of phosphorus it is clear, that its use as a material for the negative electrode of a sodium-ion battery is possible only when synthesizing various phosphorus-containing composites. The most popular composites are phosphorus-carbon ones, which can be synthesized by various methods (see e. g. the Review [1]).

Probably, the most efficient method for the synthesis of composites of phosphorus with carbon is the evaporation-condensation method [2–13], which consists in heating a mixture of phosphorus with carbon to a certain temperature, followed by gradual cooling of this mixture. In this case, the evaporation and condensation of phosphorus into carbon occurs. This method provides a stable composite of

phosphorus with carbon, and the phosphorus particles have nanometer sizes. It is precisely this method with certain modifications that was used in the previous work of our lab [14]. This paper has reported rather promising performances of composite of red phosphorus with chronopotentiometry and cyclic voltammetry. The electrode with such a composite demonstrated specific reversible capacity of 1870 mAh g^{-1} at 0.05C and 190 mAh g^{-1} at 10C (all figures were calculated per mass of phosphorus).

All measurements in [14] (as well as in all quoted references) were carried out at room temperature. At the same time, the probability of sodium-ion batteries to be used at lower temperatures is a key problem during their development. We are unaware of research of temperature effect upon sodium insertion in phosphorus-based materials. The goal we pursue in the present work (which is a natural continuation of [14]) is to study the effect of lower temperatures on the performances of phosphorus-carbon composite. A significant difference of the present work from [14] is the change in the carbon component, instead of Ketjenblack EC300J in the present work was used so-called modified oxidized graphite (MOG) [15]. MOG is some kind of layered graphite compound (or thermoexpanded graphite). Since MOG has a specific surface area less than Ketjenblack EC300J (*ca*. 100 m^2 g^{-1} *vs*. 800 m^2 g^{-1}), it was assumed that its composite with phosphorus would have a lower irreversible capacity of the first cycle than the composite of carbon black with phosphorus.

2. EXPERIMENTAL

2.1 Synthesis of the MOG.

Modified oxidized graphite was synthesized in the wake of patent [16]. A powder of natural graphite GL-1 was suspended in a mixture of concentrated aqueous solutions of nitric and sulfuric acids with minor additive of $(NH_4)ClO_4$. After aging of the reaction mixture for 16 hours it was filtered, and the precipitate was treated with $HClO_2$ with forming graphite chlorate. The final product was dried in flow of hot air. According to [15] this product consisted of globular particles sized from 20 to 50 μm, globules consisting of multilayer graphene sheets. According to [16] MOG contains up to 12–14 w/o O.

2.2 Synthesis of phosphorus–MOG composite (P@MOG)

The method of P@MOG synthesis was like that described in [14] for P@KB-EC300J composite. The mixture of commercial powders of red phosphorus (Ruskhim OJSC) and MOG (7:3) was thoroughly ground in agate mortar, and then dried under vacuum at a temperature of 110 °C. The dry mixture was placed in a hermetically sealed stainless steel capsule. This procedure was carried out in a glove box with argon atmosphere (Spectroscopic Systems LLC, Russia). The water and oxygen content in the box were less than 1 ppm. Then the capsule was placed in a tubular furnace and heat-treated at 650–670 °C for two hours. Next, the furnace was gradually cooled to room temperature for eight hours.

2.3 Characterization of P@MOG.

Similar to [14], the structure of P@MOG composite was characterized by powder X-ray diffraction (X-ray Powder Diffractometer Huber G670 with Co tube), whereas microstructure and particle morphology, as well as elemental composition were observed on a JEOL JSM 6490 LV scanning electron microscope (SEM) with an INCA energy dispersive X-ray analyzer (EDX).

2.4 Manufacture of electrodes and assembly of electrochemical cells.

All these procedures also were like described in [14]. The active material, P@MOG was mixed with an aqueous solution of carboxymethyl cellulose in the ratio (9:1, wt.%), then this mixture was ultrasonically homogenized (Sonics Vibra Cell, USA). The resulting slurry was applied to stainless steel current-collectors, dried in an air at a temperature of 80 °C and then dried under vacuum at a temperature of 120 °C for 8 hours. Electrochemical measurements were carried out in sealed three-electrode cells. The auxiliary and reference electrodes were made of sodium metal rolled onto a current-collectors of nickel foil. The area of the electrodes was 4.5 cm^2. The load of active substance (P) on the electrode was 2–3 mg cm^{-2}. Electrochemical cells were assembled in the glove box. A 1 M $NaClO_4$ solution in a mixture of propylene carbonate and ethylene carbonate (1:1, vol.) was used as an electrolyte. The water content in the electrolyte, measured using a titrator (917 Coulometer, Metrohm) was not more than 15 ppm.

The registration of galvanostatic charge-discharge curves of the P@TEG composite at low temperatures was carried out using a computerized heat-cold chamber KTKh-165-65 (Russia).

2.5 Electrochemical testing

To determine the electrochemical performances of the synthesized samples, the methods of chronopotentiometry and cyclic voltammetry were used. Galvanostatic charging-discharge curves were recorded using a multichannel computer-aided cycler AZVRIK-50-10V (Russia, Buster). The charging capacity corresponded to the insertion of sodium into the phosphorus-carbon composite, the discharge capacity corresponded to its extraction from the phosphorus-carbon composite. When determining the specific capacities, the calculation was carried out on the mass of phosphorus in the composite. Cyclic voltammograms were recorded using a multichannel potentiostat P20-X8 (Russia, Elins).

3. RESULTS AND DISCUSSION

3.1 Structure and morphology of the P@MOG composite.

Figure 1 presents the diffraction patterns of red phosphorus, MOG and synthesized P@MOG composite. On the whole these diffraction patterns are in good agreement with the results reported in [14], as well as in [7, 17] and evidence the formation of a phosphorus composite with carbon.

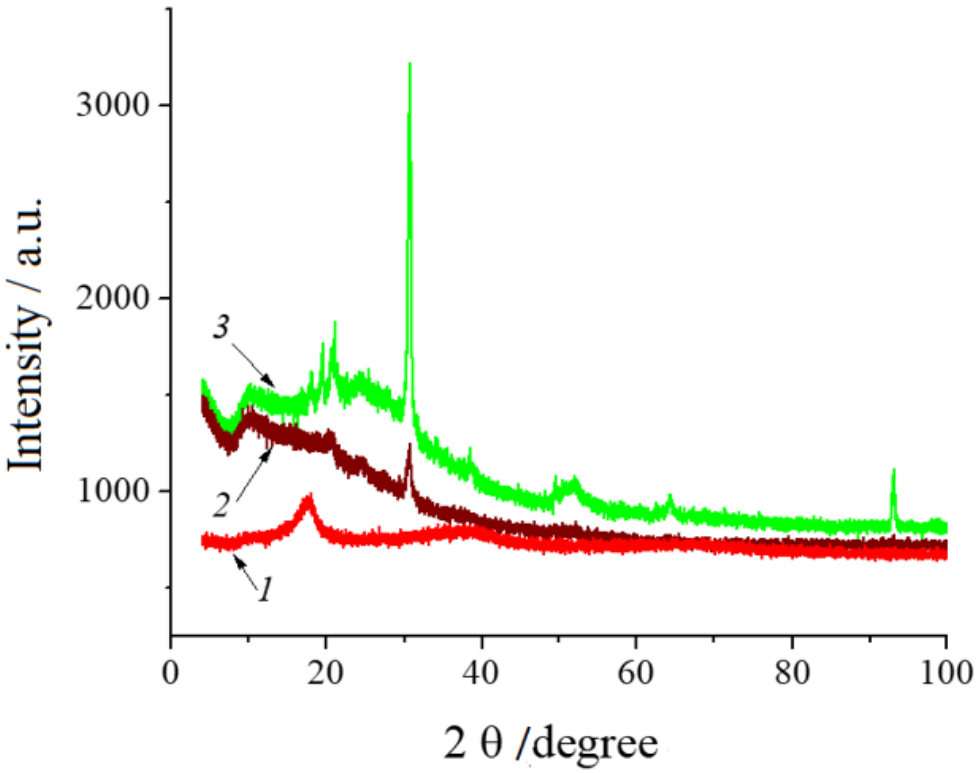

Figure 1. The diffraction patterns of red phosphorus (*1*), MOG (*2*), and P@MOG composite (*3*).

Figure 2 demonstrates the results of scanning electron microscopy of P@MOG composite. The SEM image shows certain agglomeration of individual MOG globules. The phosphorus nanoparticles cannot be seen at such magnification.

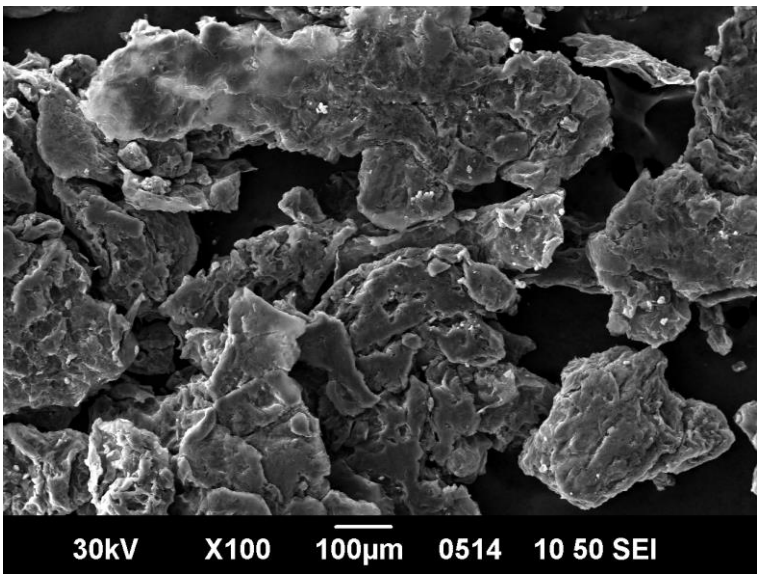

Figure 2. SEM image of P@MOG composite

Figure 3 shows EDX spectrum of P@MOG composite which confirms notable content of oxygen in MOG.

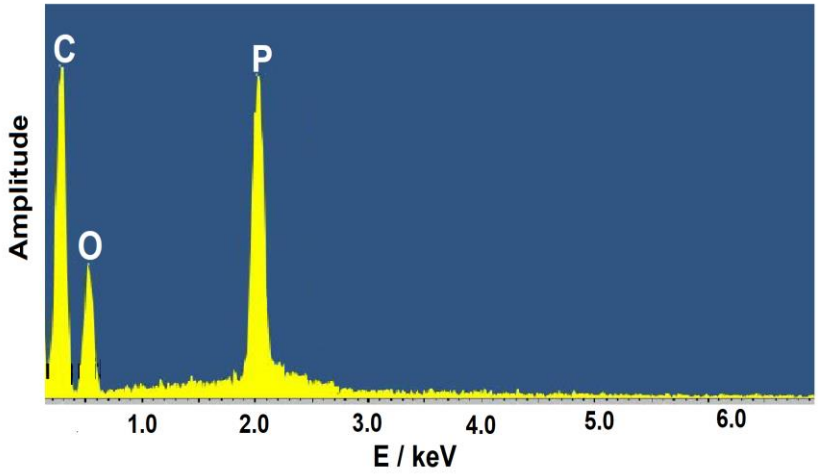

Figure 3. EDX spectrum of P@MOG composite

3.2 Room-temperature electrochemical testing of P@MOG composite

Galvanostatic charge-discharge curves of electrode based on P@MOG composite taken at C/20 (130 mA g^{-1}) are presented in Fig. 4. Qualitatively these curves agree with those reported in [14] for P@KB-EC300J composite. However, discharge capacity of P@MOG composite happens to be some less than that of P@KB-EC300J composite which can be explained by difference in carbon components in both composites. At the same time, irreversible capacity of the first cycle for electrode based on P@MOG composite was notably less than that for electrode based on P@KB-EC300J composite.

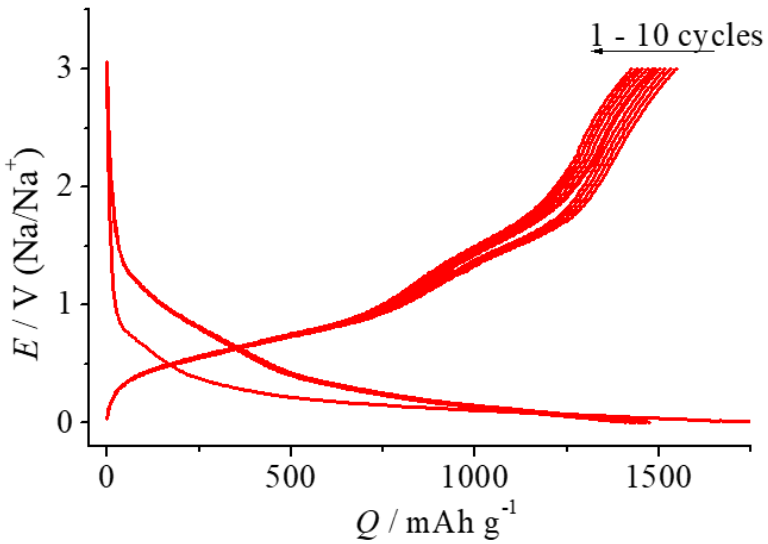

Figure 4. Galvanostatic charge-discharge curves of the initial 10 cycles for electrode based on P@MOG composite

Figure 5 demonstrates cyclic voltammograms (CVs) taken at the electrode with P@MOG composite at various potential scan rates.

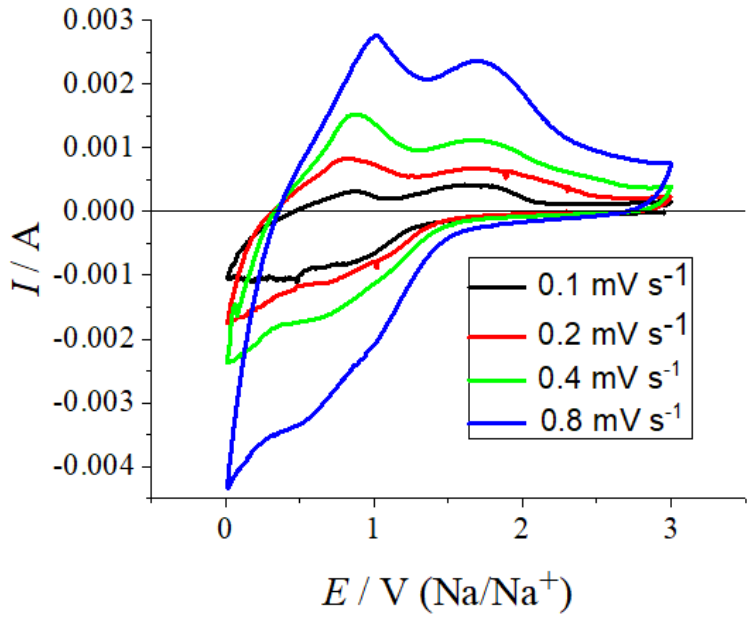

Figure 5. The cyclic voltammograms for electrode from P@MOG composite at various potential scan rates.

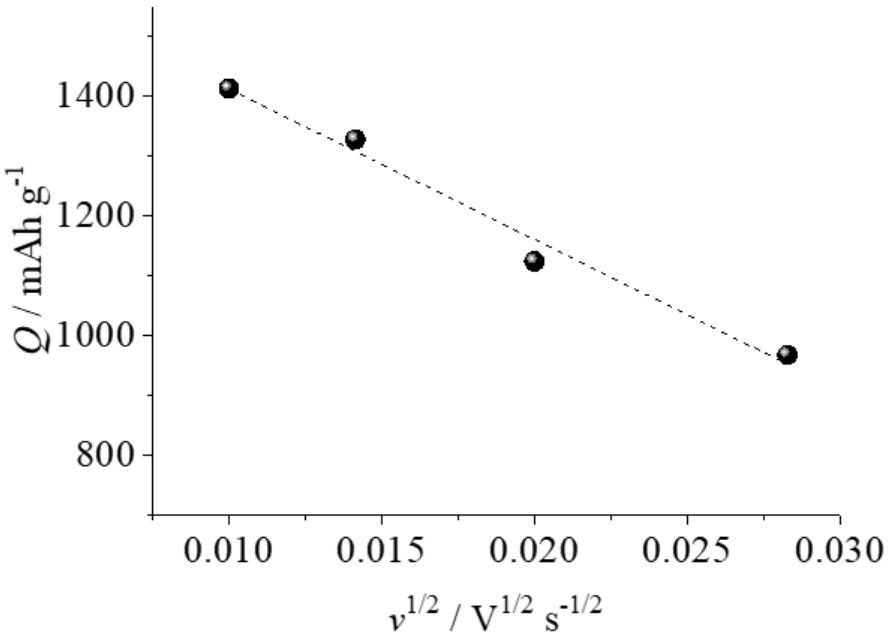

Figure 6. Discharge capacity calculated from CVs *vs* square root of potential scan rate

These CVs are in reasonable agreement with the results of galvanostatic measurements on the one hand, and with CVs reported in [14] for another phosphorus-carbon composite, on the other hand.

It is worth noting however that there is some quantitative difference between CVs taken at the P@MOG composite and at P@KB-EC300J composite. The difference of two anodic peak potentials for the former composite is by 0.3-0.4 V less than for the latter one. This points to faster sodium extraction from P@MOG composite.

The discharge capacity was calculated also by integrating CVs with due account for potential scan rate:

$$Q = \frac{1}{v} \int_{E_{init}}^{E_{fin}} i dE \qquad (1)$$

Dependence of Q thus calculated on potential scan rate is shown in Fig. 6. Linear dependence Q *vs.* $v^{1/2}$ testifies the diffusion nature of kinetics of sodium extraction. This conclusion also agrees with the data of [14].

3.3 Electrochemical testing of P@MOG composite at lower temperatures

Electrochemical testing in a wide temperature range was carried out in galvanostatic mode at a current density 260 mA g^{-1}, which corresponds to C/10. Charge-discharge curves taken at the temperatures 20, 10, 0, –10, –15, –20, –30, and –40 ºC are shown in Fig. 7. One can see that lowering temperature leads to regular decrease of discharge capacity, without notable change of shape of charge-discharge curves. In this respect the behavior of P@MOG composite is similar to that of $Na_2Ti_3O_7$@C composite [18]. (Sodium titanate is considered as a promising candidate for negative electrode of sodium-ion batteries, although with much less specific capacity than phosphorus).

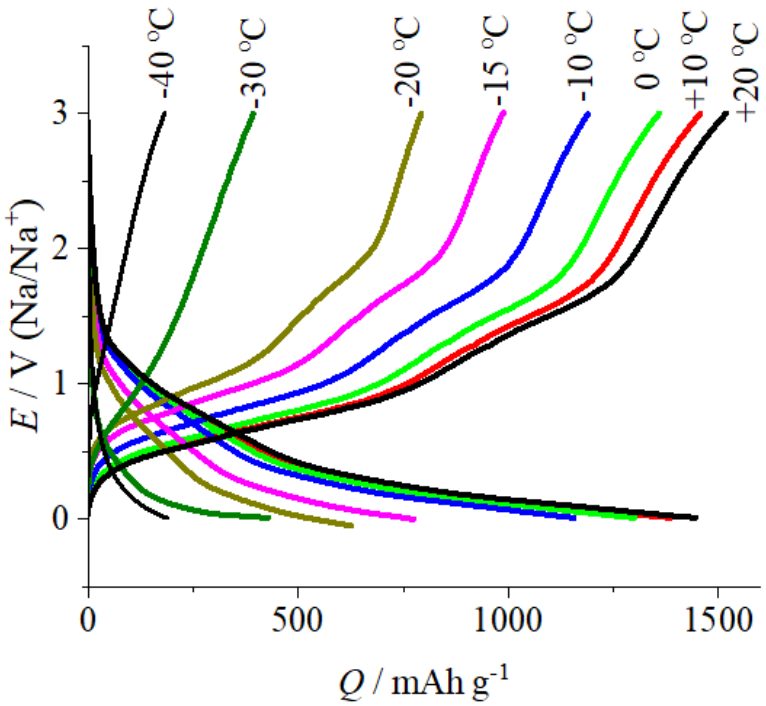

Figure 7. Galvanostatic charge-discharge curves at the electrode with P@MOG composites at the temperatures from –40 to +20 ºC at current density 250 mA g^{-1}.

Decrease of discharge capacity along lowering temperature is especially noticeable at the temperatures less than –10 °C. Indeed, lowering temperature from 20 to –10 °C resulted in the capacity diminishing by mere 20%. After following temperature decrease by 30 °C specific capacity plummeted by more than sixfold. That is why the experiments at lower temperatures were deemed inexpedient, although the freezing point of the electrolyte is *ca*. –80 °C.

Figure 8 presents temperature dependence of charge and discharge capacity of P@MOG composite in Arrhenius co-ordinates. The nature of such a presentation was discussed in length in [19] when studying lithium intercalation into graphite, as well as in [20] when studying lithium insertion into lithium titanate. It is seen that charge and discharge capacities barely differ. It is seen also that such dependence could be described by two linear sections. The slope of "high-temperature" section corresponds to effective activation energy of 4.2 kJ mole^{-1}, slope of "low-temperature" section corresponds to effective activation energy of 34 kJ mole^{-1}. The last figure is rather reasonable quantity, similar for other materials. It is worth noting that similar situation was noted in a number of works concerning temperature dependence of lithium insertion into various materials [19–21].

As an indicative characteristic of polarization in galvanostatic measurements, the potential corresponding to half-capacity is often used (see, e.g., [20–22]). Fig. 9 demonstrates such characteristic potentials for the anodic and cathodic processes at the electrode with P@MOG. The salient feature of Fig. 9 is sufficient difference between anodic and cathodic polarization. While the anodic polarization increases strongly with decreasing temperature (especially at temperatures below –10 °C), the temperature dependence of cathodic polarization is much less pronounced. This fact contrasts with the results reported in [20, 21] for the effect of temperature on polarization upon the lithium insertion into titanate and iron phosphate.

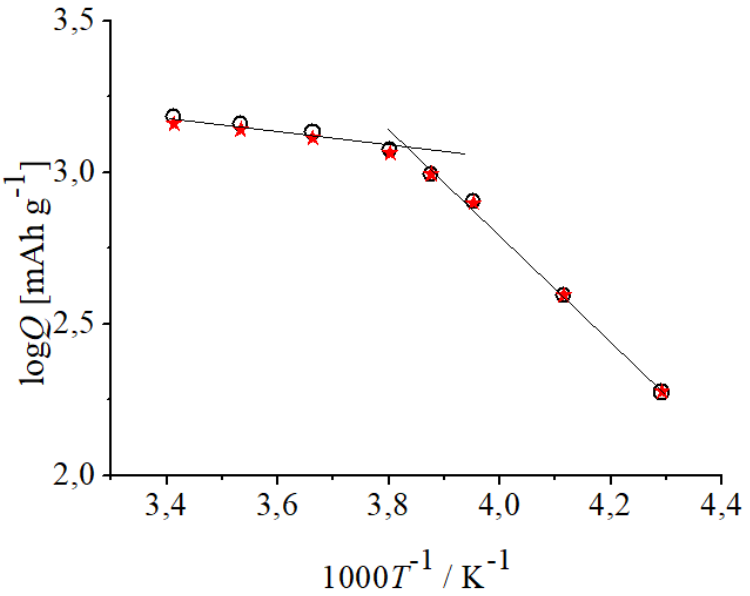

Figure 8. Temperature dependence of charge (red stars) and discharge (black circles) capacity of P@MOG composite

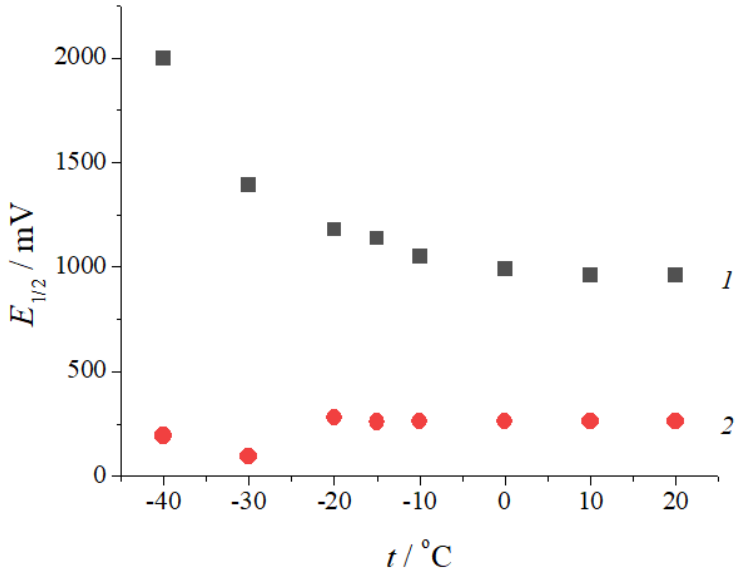

Figure 9. Temperature dependence of characteristic potential values for anodic (*1*) and cathodic (*2*) processes at P@MOG composite

4. CONCLUSION

The composite of red phosphorus with modified oxidized graphite (P@MOG) was synthesized by modified evaporation-condensation method. Electrochemical performances of the composite were studied by chronopotentiometry and cyclic voltammetry in the temperature range from –40 to +20 ºC. At room temperature the reversible charge-discharge capacity of P@MOG happened to be some less than that of composite of phosphorus with Ketjenblack EC300J studied earlier, although irreversible capacity loss of P@MOG was noticeable less than that of Ketjenblack EC300J. Lowering temperature leads to decrease of discharge capacity, especially at the most low temperatures. Discharge capacity at –10 and –40 ºC amounts to ca. 80% and 13% of room-temperature capacity.

ACKNOWLEDGEMENTS
The reported study was funded by Russian Foundation for Basic Researches (RFBR) according to the research project № 19-03-00236, and partially by the Ministry of Science and Higher Education of the Russian Federation.

References

1. T. L. Kulova and A. M. Skundin, *Russ. J. Electrochem.,* 56 (2020) 1.
2. Z. Zhu, Y. Wen, X. Fan, T. Gao, F. Han, C. Luo, S.C. Liou, C. Wang, *ACS Nano*, 9 (2015) 3254.
3. B. Ruan, J. Wang, D. Shi, Y. Xu, S. Chou, H. Liu, J. Wang, *J. Mater. Chem. A*, 3 (2015) 19011
4. W. Li, Z. Yang, M. Li, Y. Jiang, X. Wei, X. Zhong, L. Gu, Y. Yu, *Nano Lett*., 16 (2016) 1546.
5. Z. Yu, J. Song, D. Wang, D. Wang, *Nano Energy*, 40 (2017) 550.
6. J. Xu, J. Ding, W. Zhu, X. Zhou, S. Ge, N. Yuan, *Sci. China Mater.*, 61 (2018) 371.
7. Y. Liu, A. Zhang, C. Shen, Q. Liu, X. Cao, Y. Ma, L. Chen, C. Lau, T.C. Chen, F. Wei, C. Zhou,

ACS Nano, 11 (2017) 5530.
8. M. Li, N. Feng, M. Liu, Z. Cong, J. Sun, C. Du, Q. Liu, X. Pu, W. Hu, *Science Bulletin*, 63 (2018) 982.
9. Y. Wu, Z. Liu, X. Zhong, X. Cheng, Z. Fan, Y. Yu, *Small*, 14 (2018) Article No. 1703472.
10. X. Ma, L. Chen, X. Ren, G. Hou, L. Chen, L. Zhang, B. Liu, Q. Ai, L. Zhang, P. Si, J. Lou, J. Feng, L. Ci, *J. Mater. Chem. A*, 6 (2018) 1574.
11. W. Li, S. Hu, X. Luo, Z. Li, X. Sun, M. Li, F. Liu, Y. Yu, *Adv. Mater.*, 29 (2017) Article No. 1605820.
12. C. Zhang, X. Wang, Q. Liang, X. Liu, Q. Weng, J. Liu, Y. Yang, Z. Dai, K. Ding, Y. Bando, J. Tang, D. Golberg, *Nano Lett.*, 16 (2016) 2054.
13. J. Li, L. Wang, Z. Wang, G. Tian, X. He, *ACS Omega*, 2 (2017) 4440.
14. A. Skundin, D. Gryzlov, T. Kulova, Y. Kudryashova, A. Kuz'mina, *Int. J. Electrochem. Sci.*, 15 (2020) 1622.
15. T.L. Kulova, N.F. Nikol'skaya, A.M. Skundin, *Russ. J. Electrochem.,* 44 (2008) 558.
16. RF Patent No. 2198137 (2002)
17. Y. Wang, L. Tian, Z. Yao, F. Li, S. Li, S. Ye, *Electrochim. Acta*, 163 (2015) 71.
18. T. Kulova, A. Skundin, A. Chekannikov, S. Novikova, I. Stenina, Y. Kudryashova, G. Sinenko, *Int. J. Electrochem. Sci.*, 14 (2019) 1451.
19. T.L. Kulova, *Russ. J. Electrochem.*, 40 (2004) 1052.
20. E.K. Tusseeva, T.L. Kulova, and A.M. Skundin, *Russ. J. Electrochem.*, 54 (2018) 1186.
21. E.K. Tusseeva, T.L. Kulova, A.M. Skundin, A.K. Galeeva, and A.P. Kurbatov, *Russ. J. Electrochem.*, 55 (2019) 194.
22. Wu, X.-L., Guo, Y.-G., Su, J., Xiong, J.-W., Zhang, Y.-L., and Wan, L.-J., *Adv. Energy Mater.*, 3 (2013) 1155.